

DIPLODOCUS I: Framework for the evaluation of relativistic transport equations with continuous forcing and discrete particle interactions

Christopher N. Everett[✉] and Garret Cotter[✉]

Oxford Astrophysics, Denys Wilkinson Building, Keble Road, Oxford, OX1 3RH, United Kingdom

(Dated: October 15, 2025)

DIPLODOCUS (**D**istribution-**I**n-**P**lateaux **m**eth**O**ology for the **C**omp**U**tation of **t**ransport **e**quations) is a novel framework being developed for the mesoscopic modelling of astrophysical systems via the transport of particle distribution functions through the seven dimensions of phase space, including continuous forces and discrete interactions between particles. This first paper in a series provides an overview of the analytical framework behind the model, consisting of an integral formulation of the relativistic transport equations (Boltzmann equations) and a discretisation procedure for the particle distribution function (*Distribution-In-Plateaux*). The latter allows for the evaluation of anisotropic interactions, and generates a conservative numerical scheme for a distribution function's transport through phase space.

I. INTRODUCTION

The physical properties of astronomical phenomena must usually be inferred by distant observation alone. Blazars are a class of objects whose observed emissions are thought to originate from magnetised, relativistic jets of material formed close to the black holes at the centre of Active Galactic Nuclei (AGN) and directed almost exactly along our line of sight. The spectra of such objects is truly multi-wavelength, spanning from radio to ultra-high energy gamma rays, typically with a double peaked shape [1–3].

The processes that dominate this emission are generally thought to be synchrotron radiation and inverse Compton scattering from either leptonic and/or hadronic populations within the jets. The observed brightness of such processes is heavily dependent on the properties of the in-situ particle populations, therefore it is of critical importance that such processes and populations are well modelled.

Modelling of AGN jets can broadly be classified as microscopic or macroscopic. These are not completely separate as the latter is derived from the former, however their execution is sufficiently distinguishable that they may be considered separate approaches.

In deriving macroscopic (hydrodynamic) models such as (General Relativistic Magneto-)HydroDynamics (GRM)HD, particle populations are assumed to be follow some Maxwellian (thermal) distribution in momentum space, which depend on a small set of parameters, e.g. temperature, density and bulk flow velocity. This reduces the dimensionality, allowing a large spatial domains to be modelled, leading to high resolution simulations of the global jetted AGN structure [4–7] at the cost of limited information on the underlying micro-scale interactions between particle populations, hence poor direct simulation of emissions.

Microscopic (kinetic) models maintain information about the underlying distribution of particles in momentum space, at the cost of the increased dimensionality. To make this computationally tractable, other assumptions, e.g. isotropy in momentum, are often made to reduce the dimensionality as much as possible.

One frequently used microscopic approach, in the field of plasma physics, is that of Particle-In-Cell (PIC). PIC replaces particle distributions with a finite number of discrete particles that attempt to simulate the entire distribution. This approach works well when distributions are near thermal or when small scale plasma instabilities and dynamics require resolution, such as for particle acceleration in magnetised shock fronts and reconnection regions [8–11]. However, due computational limits, PIC can only simulate a finite number of particles. This limits sampling of both the distribution and interaction processes and constrains the spatial extent of any simulation. Therefore, PIC cannot typically be applied on a macro-scale.

An alternate microscopic approach is to assume symmetries in the particle distribution in space and momentum space. For example, an emitting region of an astrophysical source can be simplified to a spherical or slab-like zone or zones with an internally isotropic distribution of particles. Early astrophysical use of these methods was in modelling cosmic ray transport [12–14]. Here, in addition to spherical symmetry in momentum space, specifically with reference to a co-moving frame, particle distributions were taken to be close to Maxwellian. The assumption of isotropy in particular led to extensive work [15–25] describing a wide range of interactions between particles and fields, with only small ventures into the world of anisotropy for specific [26–29] and general [30] interactions. These works form the foundation of modern single/multi-zone models for jetted astrophysical sources [31–45], which maintain the tradition of momentum-space isotropy to limit computational requirements. These requirements are further reduced by considering additional symmetries in the spatial distribution of particles. In general, such models operate by considering independent, homogenous zones of isotropic

* Contact e-mail: christopher.everett@physics.ox.ac.uk

plasma, normally spherical or slab-like in shape, with prescribed internal properties such as bulk Lorentz factor, magnetic field strength and initial particle distributions. These zones may then be placed along the axis of the jet to generate structure, though typically zones do not interact with one another. Within these zones, the particle distributions are evolved according to their interactions and the prescribed parameters of the zone. Emission spectra are then generated by combining and Doppler boosting photon populations from each zone into an observer frame. These spectra can then be fit to observed data of astrophysical sources. These zoned model fits have provided great insight into the environment and dynamics of sources like AGN jets, allowing the study of questions such as how are particles accelerated to the initial distributions, and whether the jet material is dominated by leptonic or hadronic particles, which are still of some debate [46–48].

The insight these zoned models have provided into blazars, and jetted astrophysical sources in general, such as X-Ray Binaries (XRB) and Gamma Ray Bursts (GRBs), should not be understated, see, for example, Refs. [34, 38, 49–53]. However, zoned models are intrinsically limited by their constraining symmetries and it is yet to be seen if their results are robust upon relaxation of these assumptions.

The work described in this series of papers was spawned in an attempt to assess that robustness. If momentum-space isotropy and spatial homogeneity were eliminated from zoned models, would the simulated emissions continue to fit the observed data? If so would there be a significant deviation in terms of parametrisation of the source? In either case, would this relaxation allow for deeper understanding?

Recent work has begun to question and probe these assumptions. Studies in the fields of pair-plasma winds [54–56] and cosmic-ray propagation [57, 58] have demonstrated self-consistent evolution of axisymmetric particle distributions using microscopic approaches. This shows that the additional dimensionality associated with relaxing the assumption of isotropy is within the capability of modern computing.

Further, the axisymmetry studied by Ref. [58] provided a unique explanation for observations of a globular cluster, Terzan 5. A source of low-energy gamma rays is observed coincident with the location of the globular cluster, while a source of high-energy gamma rays is spatially displaced in the direction of Terzan 5’s magnetotail. Accelerated cosmic rays escape down this magnetotail in a narrow cone, with pitch angles not within our line of sight, so their high-energy emission is initially invisible to us. As they propagate down the magnetotail, their pitch angles begin to isotropise due to magnetic turbulence and cooling. Once sufficiently isotropic, their emissions become visible. This explanation of the observed spatial separation is only made possible by considering the evolution of both isotropic and anisotropic populations.

Without the assumption of symmetries, kinetic models boil down to a question of particle transport: how does a particle go from point *A* to point *B*? (With the slight complication that point *A* and point *B* exist not in three dimensions of space but the seven dimensions of phase space that include space, time and momentum.) This question expands beyond that of just modelling jetted astrophysical sources, and as such the range of fields this work may be applicable to is greatly expanded.

This process of particle transport includes aspects of both microscopic and macroscopic models; small scale interactions and large scale advection and spatial structure. As such it lies between these two - in the mesoscopic regime.

This first paper (Paper I) in the series aims to give an overarching description of this mesoscopic particle transport in a very general sense, forming the backbone of this work. Section II describes, in a coordinate-free way, how particles get from *A* to *B* in phase space, and what exactly that means. Section III then adds in coordinates to the description. Finally Section IV describes the methodology this work is using to solve this problem of transport. Paper II will then describe the numerical implementation of the transport defined in Paper I, with a demonstration of DIPLODOCUS’ microscopic capabilities, i.e. particle, interactions, emission and forcing. Paper III will then examine DIPLODOCUS’ macroscopic capabilities, with the inclusion of spatial structure and advection.

II. COORDINATE-FREE TRANSPORT EQUATION

This section defines (with some rigour) a coordinate-free, covariant form of the transport equations for particle distribution functions through phase space, also more generally known as Boltzmann equations [61]. The use of a coordinate-free approach is mathematically compact, and allows the transport equations to be adapted to any physical (or even non-physical) systems.

In the context of astrophysical sources, particles encounter continuous conservative (Hamiltonian) forces, such as the electromagnetic Lorentz force, as well as non-conservative (non-Hamiltonian) forces, such as radiation reaction that generates synchrotron emission. Particles may also encounter discrete, discontinuous interactions, i.e. collisions, which affect their path through phase space.

There is a rich history of developing Boltzmann equations for the purpose of astrophysical modelling. However, most derivations focus solely on conservative cases, neglecting non-conservative elements. This work primarily builds on the approaches taken by Refs. [12, 62, 63]. Other works, some derived from the above sources and some independent, that have made impressions on the work presented here include Refs. [64–74].

A. A to B: Phase Flow on a Manifold

As a first step, consider a single particle located at some point A at some instance and at B at a later instance. These points A and B exist in an abstract phase space, a differentiable manifold of dimension n , denoted by \mathcal{M} . Both points exist along an unique curve $\gamma(\lambda)$, where λ is an affine parameter along that curve such that $\gamma(\lambda_A) = A$ and $\gamma(\lambda_B) = B$. The coordinates of any point along this curve have the form $\mathbf{y} = (y^1, \dots, y^n)$ and there exists a unique vector \mathbf{v} tangent to the curve at each point. The curve $\gamma(\lambda)$ is therefore defined by the equation of motion

$$\frac{d\mathbf{y}}{d\lambda} = \mathbf{v}, \quad (1)$$

and is known as the particle's worldline through phase space (see Fig. 1).

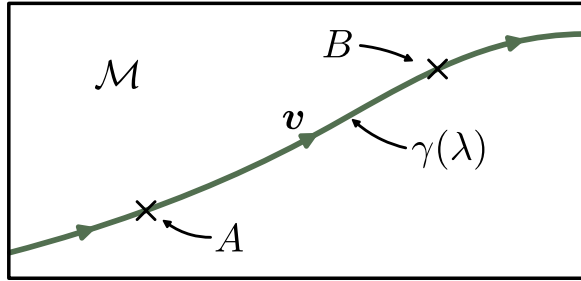


FIG. 1. The worldline of a single particle through phase space (\mathcal{M}) between two points A and B , defined by a curve $\gamma(\lambda)$, with λ being some affine parameter of that curve, and tangent to the vector \mathbf{v} .

Now consider expanding this concept to every point $q \in \mathcal{M}$, i.e. at every point there exists a vector field \mathbf{v} which defines a unique congruence of worldlines $\gamma_q(\lambda)$ that fill \mathcal{M} . These curves define how any particle will evolve if placed at any point $q \in \mathcal{M}$ (see Fig. 2).

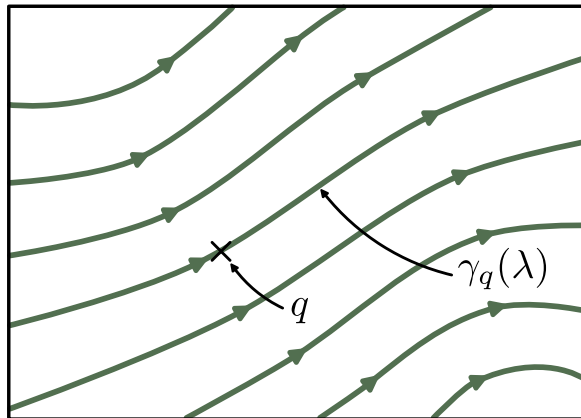


FIG. 2. A congruence of worldlines γ_q through phase space \mathcal{M} defined by the vector field \mathbf{v} at every point $q \in \mathcal{M}$.

The manifold \mathcal{M} has a volume form (volume element) associated with it defined by

$$\Omega = \Omega(\mathbf{y}) \mathbf{d}y^1 \wedge \dots \wedge \mathbf{d}y^n = \Omega(\mathbf{y}) \mathbf{d}y^{1\dots n}, \quad (2)$$

where \wedge is the wedge product and $\mathbf{d}y^{1\dots n}$ is shorthand for $\mathbf{d}y^1 \wedge \dots \wedge \mathbf{d}y^n$. The evolution of this volume form with the phase flow generated by \mathbf{v} is given by a Lie derivative with respect to \mathbf{v} (also known as the Liouville operator or vector)

$$\mathcal{L}_v \Omega = \mathbf{d}(\mathbf{v} \lrcorner \Omega) + \mathbf{v} \lrcorner (\mathbf{d}\Omega), \quad (3)$$

where Cartan's magic formula¹ has been used, with \mathbf{d} being the exterior derivative and \lrcorner being the interior product². In general, as Ω is a volume form, i.e. is a differential form of dimension n on a n dimensional manifold, $\mathbf{d}\Omega = 0$ and what remains is

$$\mathcal{L}_v \Omega = \mathbf{d}(\mathbf{v} \lrcorner \Omega) = (\text{div}_\Omega \mathbf{v}) \Omega = \mathbf{d}\omega, \quad (4)$$

where div_Ω is the Ω -divergence. Note that $\mathbf{v} \lrcorner \Omega \equiv \omega$ defines the hypersurface element for hypersurfaces in \mathcal{M} .

B. The Distribution Function

For Hamiltonian (conservative) systems, $\mathbf{d}\omega = 0$ and therefore $\mathcal{L}_v \Omega = 0$, which is a statement of Liouville's theorem [79] that the *phase space volume is invariant with respect to the phase flow*. Systems of importance to astrophysics are not in general Hamiltonian (see Section III A) and as such the phase space volume is *not*, in general, invariant with respect to the phase flow i.e. $\mathcal{L}_v \Omega \neq 0$. Hence Liouville's theorem does not apply and instead must be generalised.

Consider a new volume form $\bar{\Omega} \equiv f(\mathbf{y}) \Omega$, where f is some differentiable scalar field on \mathcal{M} , defined such that the new phase space volume element satisfies:

$$\mathcal{L}_v \bar{\Omega} = \mathcal{L}_v(f\Omega) = 0. \quad (5)$$

The condition on f for such a statement to be true may be obtained by expanding the Lie derivative using the product rule,

$$\mathcal{L}_v(f\Omega) = (\mathbf{v}(f) + f\text{div}_\Omega \mathbf{v}) \Omega = 0. \quad (6)$$

For non-trivial Ω , Eq. (6) provides a differential transport equation for f through phase space

$$\mathbf{v}(f) + f\text{div}_\Omega \mathbf{v} = 0. \quad (7)$$

¹ The “magic formula” is often associated with Élie Cartan, who demonstrates a proof in Ref. [75]; however Ref. [76] points out that formula also appears in the earlier work by Théophile De Donder [77] (verified by the author), making this a potential case for Stigler's law of eponymy [78]. Hence it is unclear who it should properly be associated with.

² The interior product is not to be confused with the inner product.

Further, the function f may be identified by considering Stokes' theorem applied to an arbitrary region of phase space $Q \in \mathcal{M}$:

$$\int_Q \mathcal{L}_v(f\Omega) = \int_Q \mathbf{d}(f\omega) = \int_{\partial Q} f\omega = 0, \quad (8)$$

where ∂Q is the bounding surface of Q . The measure $\int_{\partial Q} f\omega$ can then freely be identified with the number of worldlines (particles) passing through the closed hypersurface ∂Q , and $f\omega$ the flux of particles through ∂Q . Hence Eq. (8) simply states that the divergence in phase space of the particle flux is equal to zero, i.e. the number of worldlines (particles) entering the region Q is equal to the number leaving (see Fig. 3). Therefore f may be defined as the phase space density of worldlines (particles) on hypersurfaces in \mathcal{M} or, more colloquially, the particle distribution function.

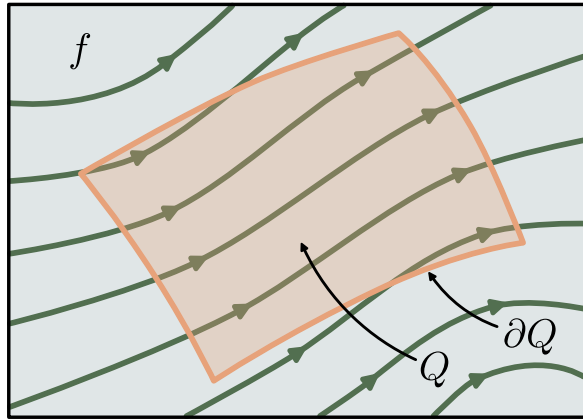


FIG. 3. Introduction of the distribution function f , a scalar field on the manifold \mathcal{M} along with an integration domain Q with volume element Ω and boundary ∂Q with hypersurface element ω . The integral $\int_{\partial Q} f\omega$ then measures the number of worldlines (particles) passing through the hypersurface ∂Q .

C. Adding Collisions

The differential and integral transport equations for the distribution function, Eqs. (7) and (8), assume an absence of discrete, discontinuous interactions (collisions) within \mathcal{M} between particles. A *collision* at a point $q \in \mathcal{M}$ may be defined as a termination or starting of a worldline (more precisely the occupation of a worldline by a particle) due to a particle being destroyed/created or receiving a discrete transfer of momentum. For example, a particle \mathfrak{a} ³ at a position $q_{\mathfrak{a}}$ in its phase space $\mathcal{M}_{\mathfrak{a}}$ may receive a discrete quantity of momentum due to scattering off a particle \mathfrak{b} at position $q_{\mathfrak{b}} \in \mathcal{M}_{\mathfrak{b}}$. The scattering

causes the termination of the worldlines of particles \mathfrak{a} and \mathfrak{b} at points $q_{\mathfrak{a}}$ and $q_{\mathfrak{b}}$ respectively as each particle's momentum (a coordinate in phase space) has changed by a discrete amount. The worldlines for particles \mathfrak{a} and \mathfrak{b} are then re-started at some new positions $q'_{\mathfrak{a}}$ and $q'_{\mathfrak{b}}$ as shown in Fig. 4. Alternatively, particle \mathfrak{a} may undergo some emissive or decay process, where again it will undergo some discrete change in momentum and therefore terminate and re-start its worldline, while also starting new worldlines for any secondary particles emitted. Interactions, scattering, collisions, emissive and decay process all have the same effect in phase space, that being the termination and starting of worldlines, hence the term *collision* will be used to refer collectively to these processes.

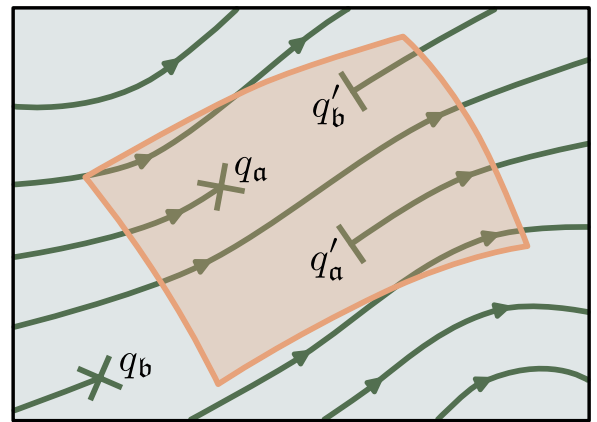


FIG. 4. Collisions (discrete transfers of momentum) are described by the termination (crosses) and starting (bar) of particle worldlines within phase space. Here a particle \mathfrak{a} at a position $q_{\mathfrak{a}}$ collides with a particle \mathfrak{b} at a position $q_{\mathfrak{b}}$, terminating each worldline. The locations $q_{\mathfrak{a}}$ and $q_{\mathfrak{b}}$ need not be coincident as the particles may have different momenta (a coordinate in phase space). The collision may cause a discrete exchange of momentum, whereby the particles then re-appear at points $q'_{\mathfrak{a}}$ and $q'_{\mathfrak{b}}$, starting a new pair of worldlines. The integral $\int_Q \mathbf{C}$ then counts the number of collisions (worldlines that are started and/or terminated) within the volume Q .

These collisions can then be represented by a new measure $\mathbf{C}(\mathbf{y}) \propto \Omega$ known as the collision integral, which “counts” the number of collisions within the volume Q (see further in Section III C). This measure can therefore be simply added to the right hand side of Eqs. (7) and (8), to give the differential transport equations for f :

$$\mathbf{v}(f) + f \text{div}_{\Omega} \mathbf{v} = \mathbf{C}. \quad (9)$$

and its integral form:

$$\int_{\partial Q} f\omega = \int_Q \mathbf{C}. \quad (10)$$

³ Particle species are referred to by Gothic scripts in this paper.

III. COORDINATE-DEPENDENT TRANSPORT EQUATION

A. Phase Flow with Coordinates

Though Eqs. (9) and (10), are mathematically elegant in their coordinate-free form, some definition of coordinates (basis vectors) are needed to give them utility in modelling astrophysical sources.

For this purpose, two sets of basis vectors are used. The nature of spacetime is assumed to be a 4D Riemannian manifold \mathcal{N} , with signature $(- + + +)$, and a coordinate basis e_α (Greek scripts) with coordinates $x^\alpha = \{x^0, \dots, x^3\}$ ⁴. For momentum space, which exists in the tangent space $T_{\mathcal{N}}$ to \mathcal{N} , a local-orthonormal basis (tetrad) e_a (Latin scripts), with components $p^a = \{p^0, \dots, p^3\}$ is used. The worldline of a particle through the 8-dimensional phase space is then given by

$$\frac{dx^\alpha}{d\lambda} = p^a e_a^\alpha, \quad \frac{dp^a}{d\lambda} = -\Gamma_{bc}^a p^b p^c + mF^a, \quad (11)$$

where the transformation between the two basis is $e_a = e_a^\alpha e_\alpha$, Γ_{bc}^a are the connection coefficients in the local orthonormal basis (i.e. Ricci rotation coefficients) and F^a are the components of some arbitrary four-force \mathbf{F} . For massive particles $m \neq 0$ the affine parameter λ is related to the proper time τ by $m\lambda = \tau$. The manifold \mathcal{M} , corresponding to the 8-dimensional phase space, is given by the set

$$\mathcal{M} = \{(\mathbf{x}, \mathbf{p}) : \mathbf{x} \in \mathcal{N}, \mathbf{p} \in T_{\mathcal{N}}, \mathbf{p}^2 \leq 0, \mathbf{p} \text{ future directed}\}. \quad (12)$$

The phase flow in \mathcal{M} is generated by the Lie derivative with respect to \mathbf{v} , where, using Eq. (11)

$$\mathbf{v} = p^a e_a^\alpha \frac{\partial}{\partial x^\alpha} + (-\Gamma_{bc}^a p^b p^c + mF^a) \frac{\partial}{\partial p^a}. \quad (13)$$

The rest mass of a particle

$$-m^2 = \mathbf{p}^2 = g_{\alpha\beta} e_a^\alpha e_b^\beta p^a p^b, \quad (14)$$

is a scalar function on \mathcal{M} which, on physicality grounds, should be a constant with respect to the phase flow i.e.

$$\mathcal{L}_v(-m^2) = 0. \quad (15)$$

Via direct calculation⁵, this yields the following constraint on the force \mathbf{F} :

$$\mathbf{F} \cdot \mathbf{p} = 0, \quad (17)$$

⁴ The choice of a precise set of coordinates, e.g. Cartesian, Cylindrical, Spherical, Schwarzschild, Boyer-Lindquist, etc. remains arbitrary. As such this model can be applied to a wide range of spacetimes.

⁵ This requires the additional relation between the connection coefficients in a orthonormal basis Γ_{bc}^a (Ricci rotation coefficients) and those in a coordinate basis $\Gamma_{\beta\gamma}^\alpha$ (Christoffel symbols):

$$\Gamma_{bc}^a = e_a^\alpha e_c^\gamma (\partial_\gamma e_b^\alpha + \Gamma_{\beta\gamma}^\alpha e_b^\beta). \quad (16)$$

which is met for all forces expected to occur within an astrophysical setting (e.g. Lorentz and radiation reaction forces). With m^2 being constant with respect to the phase flow, particles exist only on hypersurfaces in \mathcal{M} defined by $m^2 = \text{const}$. This restricted manifold is now denoted \mathcal{M}_m and is 7-dimensional with coordinates $x^\alpha = \{x^0, \dots, x^3\}$ and $p^i = \{p^1, \dots, p^3\}$, where second-half Latin alphabet letters refer to indices valued $i \in \{1, 2, 3\}$, where p^0 , the “energy” of the particle, has been chosen to be the dependent variable defined by

$$p^0 = \sqrt{m^2 + (p^i)^2}. \quad (18)$$

The phase flow on the restricted manifold \mathcal{M}_m is then given by

$$\mathbf{v} = p^a e_a^\alpha \frac{\partial}{\partial x^\alpha} + (-\Gamma_{bc}^i p^b p^c + mF^i) \frac{\partial}{\partial p^i}. \quad (19)$$

What are the volume forms on \mathcal{M}_m ? The spacetime volume form is given by the standard form⁶

$$\chi = \frac{\chi_{\alpha\beta\gamma\delta}(\mathbf{x})}{4!} dx^{\alpha\beta\gamma\delta}, \quad (20)$$

where $\chi_{\alpha\beta\gamma\delta}$ are components of the completely antisymmetric Levi-Civita tensor, with $\chi_{1234} = \sqrt{-\det(g_{\alpha\beta})} = \sqrt{-g}$. The momentum space volume, restricted to \mathcal{M}_m , is likewise given by

$$\pi = 2\Theta(p^0)\delta(\mathbf{p}^2 - m^2)\sqrt{-\eta} dp^{0123} = \frac{\sqrt{-\eta}}{p^0} dp^{123}, \quad (21)$$

where η_{ab} is the metric in momentum space. For an orthonormal basis $\sqrt{-\eta} = \sqrt{-\det(\eta_{ab})} = 1$, hence

$$\pi = \frac{1}{p^0} dp^{123} = \frac{\pi_{ijk}}{3!} dp^{ijk}. \quad (22)$$

The total volume form is then given by the wedge product of Eqs. (20) and (22):

$$\Omega = \chi \wedge \pi. \quad (23)$$

From Eq. (23), the hypersurface element ω orthogonal to the phase flow \mathbf{v} (Eq. (19)) in \mathcal{M}_m can also be evaluated:

$$\begin{aligned} \omega \equiv \mathbf{v} \lrcorner \Omega &= p^a e_a^\alpha \frac{\chi_{\alpha\beta\gamma\delta}(\mathbf{x})}{3!} dx^{\beta\gamma\delta} \wedge \pi \\ &+ \chi \wedge (-\Gamma_{bc}^i p^b p^c + mF^i) \frac{\pi_{ijk}}{2!} dp^{jk}. \end{aligned} \quad (24)$$

As discussed in Section II B, for a system to be obey Liouville’s theorem $\mathbf{d}\omega \stackrel{!}{=} 0$, by consideration of Eq. (24) this condition is equivalent to $\frac{\partial F^a}{\partial p^a} \stackrel{!}{=} 0$. As an example where this condition is met, the Lorentz force on a particle of charge q and mass m is given by

⁶ The Hodge dual of the unit function $\chi = \star 1$.

$F^a = \frac{q}{m} F^{ab} p_b$, where F^{ab} is the electromagnetic field tensor, therefore $\frac{\partial F^a}{\partial p^a} = F_a^a = 0$ as F^{ab} is antisymmetric. However, a counter example is the radiation reaction force⁷ experienced by a charged particle being accelerated by an electromagnetic field where $F^a \propto \left(\eta^{ab} + \frac{p^a p^b}{m^2 c^2} \right) \left(\frac{q}{m} p^d p^c \partial_c F_{bd} + \frac{q^2}{m^2} q F_{bc} F^{cd} p_d \right)$, for such a force it can be shown that $\frac{\partial F^a}{\partial p^a} \neq 0$, and is therefore a non-conservative force, evident by the fact that it results in the charged particle losing energy over time.

As such, non-conservative forces, such as radiation reaction, are a necessary inclusion of any self-consistent astrophysical model, hence $d\omega \neq 0$ in general and the correct forms for the transport equation for the particle distribution function are Eqs. (9) and (10).

B. Stationary Observers

It is important to define a set of observers with respect to whom the distribution function and its derived properties are measured. *If the spacetime is stationary*, it permits a set of Eulerian observers. Their worldlines are defined everywhere by the timelike unit vector $\mathbf{n} = n_\alpha e^\alpha = n_0 dt$, with $\mathbf{n} \cdot \mathbf{n} = n^0 n_0 = -1$. At each value of proper time τ along the worldline of an observer, there exists a unique, spacelike hypersurface Σ_τ orthogonal to the worldline. This hypersurface defines the set of events that are considered simultaneous with respect to that observer at that value of proper time.

The hypersurface element ω , given by Eq. (24), may be decomposed into hypersurface elements of simultaneous and non-simultaneous events as measured by a stationary observer:

$$\begin{aligned} \omega = & \left[(-p^a n_a) n^\alpha \frac{\chi_{\alpha\beta\gamma\delta}(\mathbf{x})}{3!} dx^{\beta\gamma\delta} \wedge \boldsymbol{\pi} \right] \\ & + \left[(p^a e_a^\alpha + p^a n_a n^\alpha) \frac{\chi_{\alpha\beta\gamma\delta}(\mathbf{x})}{3!} dx^{\beta\gamma\delta} \wedge \boldsymbol{\pi} \right] \\ & + \chi \wedge (-\Gamma^i_{bc} p^b p^c + m F^i) \frac{\pi_{ijk}}{2!} dp^{jk} \end{aligned} \quad (25)$$

$$= \omega_\Sigma + \omega_\Lambda.$$

The first square bracketed term in Eq. (25) is ω_Σ , referring to the element of Σ hypersurfaces, while the second square bracket is the element of timelike hypersurfaces Λ of non-simultaneous events, ω_Λ (see Fig. 5).

With a set of observers, the total number of particles in the system can be counted in a well defined way. Consider the insight from Section II B, that the $\int_{\partial Q} f\omega$ is the number of worldlines passing through some hypersurface defined by the boundary ∂Q . Therefore, taking ∂Q to

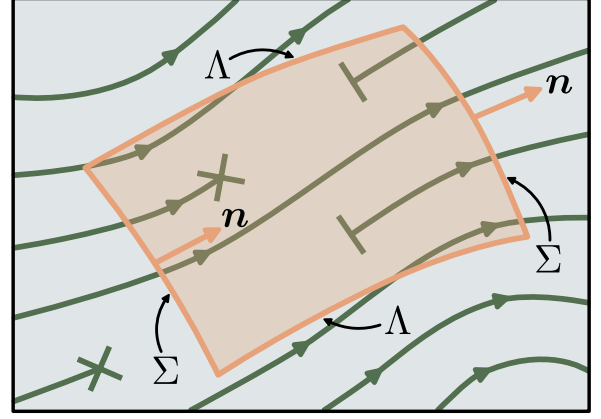


FIG. 5. Timelike Σ and spacelike Λ hypersurfaces in phase space \mathcal{M}_m defined by a set of stationary observers with trajectory tangent to \mathbf{n} . The spacelike hypersurfaces Σ define a set of simultaneous events as measured by the observer.

be the open hypersurface Σ , $\int_\Sigma f\omega = N$ the number of particles measured simultaneously passing through that surface, i.e. the total number of particles within the manifold at a given time τ according to that local observer. If $\Sigma = X \times P$ is decomposed into the product of a spatial submanifold X and the momentum-space submanifold P this integral can be expanded as

$$N = \int_\Sigma f\omega_\Sigma = \int_X -n_a n^\alpha \frac{\chi_{\alpha\beta\gamma\delta}(\mathbf{x})}{3!} dx^{\beta\gamma\delta} \int_P f p^a \boldsymbol{\pi}. \quad (26)$$

The latter part of Eq. (26) can be identified as the first moment of the distribution function i.e. locally measured 4-flow vector:

$$N^a = \int_P f p^a \boldsymbol{\pi}, \quad (27)$$

from which the scalar number density of particles n as measured by a stationary observer can be defined:

$$n = -n_a N^a. \quad (28)$$

Higher moments of the distribution function can similarly be defined, for example the locally measured stress-energy tensor is defined by

$$T^{ab} = \int_P f p^a p^b \boldsymbol{\pi}, \quad (29)$$

through which the scalar energy density $e = n_a n_b T^{ab}$ and pressure $p = \frac{1}{3} T^{ab} \Delta_{ab}$ (where $\Delta_{ab} = \eta_{ab} + n_a n_b$ is the projection tensor) can be defined.

An alternative to the set of Eulerian observers is a set of observers co-moving with some bulk flow. However, for co-moving observers, their local tetrad e_a is a function of the bulk flow, and therefore variable, unlike a Eulerian observer whose tetrad is fixed. This results in

⁷ The radiation reaction force is also known as the Abraham-Lorentz-Dirac force [80–82] [see also 83, 84, for more modern descriptions].

the hypersurface elements Eq. (24) also becoming a function of the flow and therefore so too would the numerical fluxes (see Section IV B) used to evaluate transport of the distribution function, thereby requiring unnecessary recalculation when the bulk flow changes.

C. The Collision Integral

The collision integral $\mathbf{C}(\mathbf{x}, \mathbf{p})$ is a measure of the number of worldlines that are terminated and started within some volume of phase space. It is useful to relate this to the transition probability w_{if} for an initial state i of particles to transition to a final state f . Modifying the results of [85], the differential transition probability may be written:

$$w_{if} = \delta^{(4)}(\mathbf{p}_i - \mathbf{p}_f) |T_{if}|^2 \chi, \quad (30)$$

where the Dirac delta function describes conservation of momentum during the transition and T_{if} is the standard scattering T -matrix.

Given a distribution of particles $f(\mathbf{x}, \mathbf{p})$, the number of particle worldlines crossing a Σ hypersurface is given by Eq. (26). Assuming a well defined basis transformation such $n_a = (-1, 0, 0, 0)$, this may be integrated over a test region in the spatial sub-manifold X , giving

$$\int_X \omega_\Sigma = p^0 V \pi, \quad (31)$$

where V is some spatial volume. As such the expression $p^0 V \pi$ can be thought of as the momentum-space number density of particles with a unity distribution function, i.e. 1 particle per unit hypersurface element. The differential transition probability, Eq. (30), may then be expanded to include the incident and final particle's momentum states:

$$w_{if} = \delta^{(4)}(\mathbf{p}_i - \mathbf{p}_f) \frac{|T_{if}|^2}{n_i! n_f!} \chi \prod_{a \in i} p_a^0 V \pi_a \prod_{b \in f} p_b^0 V \pi_b, \quad (32)$$

where n_i and n_f are the number of identical initial and identical final states respectively, which are included to avoid over counting states.

In the literature, the factors of $p^0 V$ are often absorbed into the scattering matrix T_{if} to generate the more familiar scattering matrix M_{if} i.e.

$$M_{if} = T_{if} \sqrt{\prod_{a \in i} p_a^0 V \prod_{b \in f} p_b^0 V}, \quad (33)$$

giving

$$w_{if} = \delta^{(4)}(\mathbf{p}_i - \mathbf{p}_f) \frac{|M_{if}|^2}{n_i! n_f!} \chi \prod_{a \in i} \pi_a \prod_{b \in f} \pi_b. \quad (34)$$

The number of worldlines terminated or started by an collision $i \rightarrow f$ is then given by reintroducing non-unity distribution functions for the initial particles:

$$N_{if} = \delta^{(4)}(\mathbf{p}_i - \mathbf{p}_f) \frac{|M_{if}|^2}{n_i! n_f!} \chi \prod_{a \in i} f_a(\mathbf{x}, \mathbf{p}) \pi_a \prod_{b \in f} \pi_b. \quad (35)$$

With the volume element for phase space given by Eq. (23), it can be recognised that the quantity N_{if} is proportional to Ω , and therefore related to the collision integral $\mathbf{C}(\mathbf{x}, \mathbf{p})$. To understand this relation, consider a particle of type- a . The number of its worldlines terminated by collisions where it is a member of the incident state i is given by $\sum_{a \in i} N_{if}$, and similarly the number of its worldlines that are started is $\sum_{a \in f} N_{if}$. The nature of the collision integral for a single particle of type- a is therefore

$$\mathbf{C}(\mathbf{x}, \mathbf{p}_a) = \sum_{a \in f} N_{if} - \sum_{a \in i} N_{if}. \quad (36)$$

Specific examples of the collision integral for binary (scattering) collisions i.e. $ab \rightarrow cd$ and emission (decay) processes i.e. $a \rightarrow bc$ are given in Appendix A.

Eq. (36) contains integrals over the momentum states of all the initial and final state particles, therefore it is of high dimensionality and further complicated by potentially non-linear dependence on the particle distribution functions. As such, it is generally impractical to use in this form unless some methodology for simplifying the integral is applied, or some assumptions are made for the symmetries of f in momentum space - traditionally, isotropy.

IV. DISTRIBUTION-IN-PLATEAUX

The integrated form of the Boltzmann equations (Eq. (10)), is mathematically elegant but in its present form is difficult to evaluate. The difficulty arises from the integrals over the entire volume of phase space. This can be simplified by splitting the integration domain Q into a set of continuous sub-domains with common boundaries. Therefore the left hand side of Eq. (10) describes the flux of particle worldlines through the boundaries of each sub-domain, while the right hand side counts collisions within each sub-domain. As all boundaries are shared between sub-domains, the number of particle worldlines is conserved over the whole domain.

To aid in simplifying the equations in this section, the set of spacetime coordinates will be denoted by $x^\alpha = \{x^0, x^1, x^2, x^3\} = \{t, x, y, z\}$, making the time coordinate t explicit, and spatial coordinates $\{x, y, z\}$ refer, abstractly, to any set of three chosen spatial coordinates not just the standard Cartesian set i.e. $\{x, y, z\}$ (see Appendix B for examples). For momentum-space, coordinates are concretely defined to be $p^i = \{p^1, p^2, p^3\} = \{p, u, \phi\}$ the set of modified spherical coordinates ($u =$

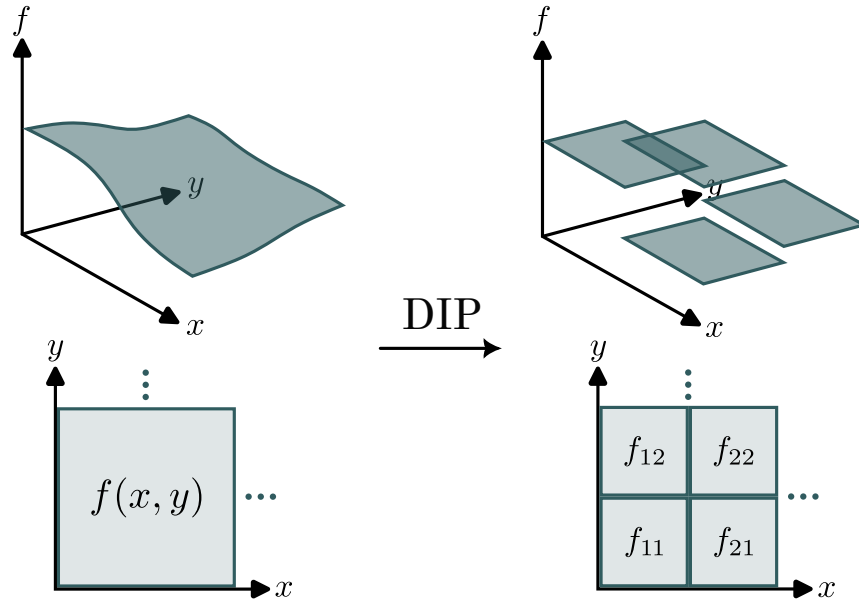


FIG. 6. The continuous distribution function f for each particle is discretised via Eq. (37) to form a range of plateaux over phase space (here taken to be two dimensional with coordinates x and y) indexed by the values f_{ij} , hence the name Distribution-In-Plateaux.

$\cos \theta$), as this is the set used for the numerical evaluation of collision integrals in [Paper II](#).

With these coordinate sets, the procedure for splitting the integration domain Q into a continuous set of sub-domains can formally be achieved by taking the particle distribution function to be constant within each sub-domain of phase space. The total distribution is formed by the sum of these constant regions⁸:

$$f(\mathbf{x}, \mathbf{p}) = \sum_{\alpha \beta \gamma \delta ijk} \frac{f_{\alpha \beta \gamma \delta ijk}}{p^2 \Delta p_i \Delta u_j \Delta \phi_k} H_\alpha(t) H_\beta(x) \times H_\gamma(y) H_\delta(z) H_i(p) H_j(u) H_k(\phi), \quad (37)$$

where H is a boxcar function and $\alpha, \beta, \gamma, \delta, i, j$ and k now refer to a discrete set of phase-space coordinates. As an example, for the t coordinate the function H is defined as

$$H_\alpha(t) = \Theta(t - t_\alpha) - \Theta(t - t_{\alpha+1}) = \begin{cases} 1, & \text{for } t_\alpha < t < t_{\alpha+1}, \\ h_\alpha^- & \text{for } t = t_\alpha \\ h_\alpha^+ = 1 - h_\alpha^- & \text{for } t = t_{\alpha+1} \\ 0, & \text{for all other } t, \end{cases} \quad (38)$$

with Θ being the Heaviside step function and h_α^\pm being the boxcar function values at the bounds of the domain $t_\alpha \leq t \leq t_{\alpha+1}$ ⁹.

Through the action of Eq. (37), the continuous distribution function is replaced by a series of plateaux, each with a “height” of $f_{\alpha \beta \gamma \delta ijk}$ over a discrete sub-domain in phase space (see Fig. 6), and hence termed “Distribution-In-Plateaux” (DIP). This nomenclature has similarities with that of the “Particle-In-Cell” (PIC), whereby the distribution function is considered as a sum over Dirac delta functions.

The factor of $p^2 \Delta p_i \Delta u_j \Delta \phi_k$ in Eq. (37) is not strictly required, rather it has been introduced for convenience such that according to Eq. (28) the scalar number density n of particles measured by the stationary observer, within a spatial sub-domain $X_{\beta \gamma \delta}$ and between times t_α and $t_{\alpha+1}$, is given by

$$n = \sum_{ijk} f_{\alpha \beta \gamma \delta ijk}, \quad (39)$$

and as such $f_{\alpha \beta \gamma \delta ijk}$ can be recognised as the number density of particles within a momentum space sub-domain P_{ijk} .

⁸ It has been noted to the authors that this method of discretisation for particle transport may be mapped to a zeroth-order discontinuous Galerkin method, which was developed independently of this work, and further, has been shown to have good conservative properties for number density and energy (see, for example, Refs. [41, 86, 87]).

⁹ By allowing the definition of $\Theta(0)$ to be a variable between 0 and 1, usually taken to be 0,1 or 1/2, modification of the numerical scheme may be made, as described in [Paper II](#), while maintaining conservative particle transport.

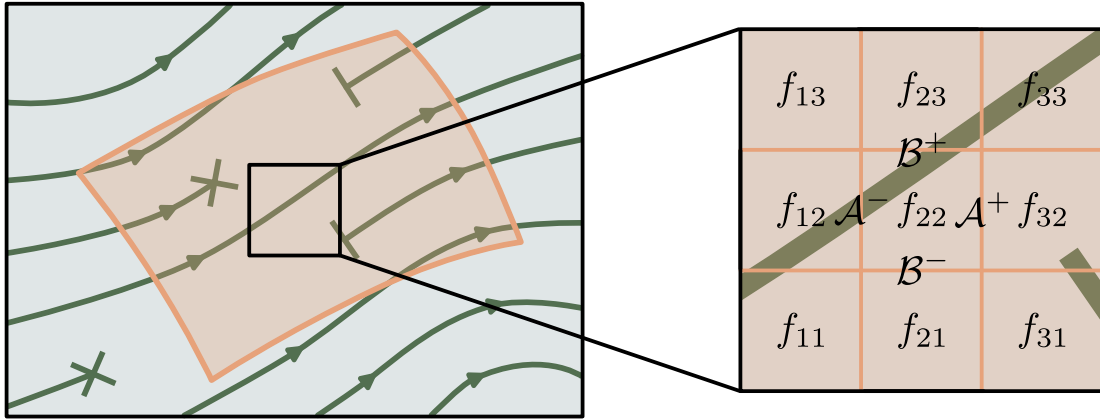


FIG. 7. Simplified schematic of how DIP applies to phase space transport (here phase space has been reduced to two dimensions). The action of Distribution-In-Plateaux Eq. (37), is to discretise phase space into sub-domain in which the distribution function f takes a single value (f_{ij} here). The left hand side of the transport equation Eq. (10) $\int_{\partial Q} f \omega$ is then an integral over the boundaries of these sub-domains, which generates the fluxes between sub-domains (\mathcal{A} and \mathcal{B} here). For this two dimensional example, the the transport equation for f_{22} takes the form $\int_{\partial Q_{22}} f \omega = (h_{32}^- f_{32} + h_{22}^+ f_{22}) \mathcal{A}^+ + (h_{22}^- f_{22} + h_{12}^+ f_{12}) \mathcal{A}^- + (h_{23}^- f_{23} + h_{22}^+ f_{22}) \mathcal{B}^+ + (h_{22}^- f_{22} + h_{21}^+ f_{21}) \mathcal{B}^-$, where the h terms (Eq. (38)) dictate the value of the distribution function on sub-domain boundaries.

A. DIP Applied to Collision Integrals

Before describing how the DIP simplifies the larger problem of phase space transport. Consider how it simplifies the problem of evaluating collision integrals. For a binary collisions $\mathbf{ab} \rightarrow \mathbf{cd}$, the gain of particles of type- \mathbf{c} is given by the collision integral (Eq. (36)):

$$\int \mathbf{C}(\mathbf{x}, \mathbf{p}_c) = \int f_a(\mathbf{x}, \mathbf{p}_a) f_b(\mathbf{x}, \mathbf{p}_b) G_{ab \rightarrow cd} d^3 p_a d^3 p_b d^3 p_c \chi, \quad (40)$$

where $G_{12 \rightarrow 34}$ is the “gain term” given by Eq. (A5). The integration domain for this term is the phase space of particle \mathbf{c} and the momentum space of particles \mathbf{a} and \mathbf{b} . By deploying DIP, the value of the distribution functions of particles \mathbf{a} , \mathbf{b} , and \mathbf{c} become constant within a sub-domains of phase space and, therefore, can be taken outside integrals over those sub-domains. Consider a momentum-space sub-domain for particle \mathbf{c} to be $P_{ijk} = [p_i, p_{i+1}] \times [u_j, u_{j+1}] \times [\phi_k, \phi_{k+1}]$, with DIP deployed, the collision integral (Eq. (40)) over this sub-domain becomes:

$$\int_{t_\alpha}^{t_{\alpha+1}} \int_{X_{\beta\gamma\delta}} \int_{P_{ijk}} \mathbf{C}(\mathbf{x}, \mathbf{p}_c) = \sum_{lmnopq} f_{a,\alpha\beta\gamma\delta lmn} \times f_{b,\alpha\beta\gamma\delta opq} G_{ab \rightarrow cd, i j k l m n o p q} \mathcal{V}_{\alpha\beta\gamma\delta}, \quad (41)$$

where the gain term has become a 9-dimensional “gain array” $G_{ab \rightarrow cd, i j k l m n o p q}$ given by Eq. (A7), and $\mathcal{V}_{\alpha\beta\gamma\delta}$ is the spacetime volume element given by Eq. (C13). The elements of the gain array are integrals over different momentum-space sub-domains of the incoming and outgoing particles, which, being independent of the distribution of those particles, are pre-computable by numerical means (see Paper II), and are proportional to the

rate of a collision. Further, elements of the gain array are independent of spatial coordinates, due to the use of a local-orthonormal basis for momentum space, and as such are valid at all points in spacetime, independent of the spacetime’s nature. This process of discretisation and integration can be applied to all collision terms equally, thereby all collisions are presented as pre-computed arrays within the DIPLODOCUS framework.

The application of DIP to collision integrals presents some immediate advantages of using DIP over PIC. As all collision array terms may be pre-evaluated and reused over multiple simulations of phase-space transport, there is a reduction in computational intensity compared to the calculation of collisions during transport - especially when the number of particles (collisions) is large. In addition, it provides uniform sampling of collisions over the entire phase-space domain - independent of the number of particles in the system.

B. DIP Applied to Transport

Consider an arbitrary but stationary spacetime, with a metric tensor given by:

$$\begin{aligned} g = & \left(-A^2 + \frac{E^2}{B^2} + \frac{F^2}{C^2} + \frac{G^2}{D^2} \right) dt \otimes dt \\ & + B^2 dx \otimes dx + C^2 dy \otimes dy + D^2 dz \otimes dz \\ & + 2E dt \otimes dx + 2F dt \otimes dy + 2G dt \otimes dz, \end{aligned} \quad (42)$$

Being stationary, the functions A, B, C, D, E, F , and G are functions of a subset of the spatial coordinates x^i only. The functions E, F, G form what is conventionally known as the *shift vector* $\beta_i = (E, F, G)$ with the function A being the *lapse function*. The metric given by Eq. (42)

could refer to a wide range of metrics commonly applied to astrophysical settings, an example subset of which are given in Appendix B.

The spacetime volume element (Eq. (42)) of the metric given by Eq. (42) has the simple form:

$$\chi_{0123} = ABCD, \quad (43)$$

and a natural coordinate transform to the tetrad of a stationary (Eulerian) observer $\mathbf{n} = -A\mathbf{dt}$, could be written:

$$e_a^\alpha = (n^\alpha, X^\alpha, Y^\alpha, Z^\alpha), \\ = \begin{pmatrix} \frac{1}{A} & -\frac{E}{AB^2} & -\frac{F}{AC^2} & -\frac{G}{AD^2} \\ 0 & \frac{\dot{X}_1}{B} & \frac{\dot{X}_2}{C} & \frac{\dot{X}_3}{D} \\ 0 & \frac{\dot{Y}_1}{B} & \frac{\dot{Y}_2}{C} & \frac{\dot{Y}_3}{D} \\ 0 & \frac{\dot{Z}_1}{B} & \frac{\dot{Z}_2}{C} & \frac{\dot{Z}_3}{D} \end{pmatrix}, \quad (44)$$

where $X^\alpha = (0, \frac{X_1}{B}, \frac{X_2}{C}, \frac{X_3}{D})$, $Y^\alpha = (0, \frac{Y_1}{B}, \frac{Y_2}{C}, \frac{Y_3}{D})$, and $Z^\alpha = (0, \frac{Z_1}{B}, \frac{Z_2}{C}, \frac{Z_3}{D})$ are a set of mutually orthonormal vectors, which are also orthogonal to \mathbf{n} . It is often standard to align \mathbf{X} , \mathbf{Y} , and \mathbf{Z} to the $\{x, y, z\}$ coordinate directions, however, they have here been left general as it can be useful to align them to some other set of vectors e.g. the local magnetic and electric field directions [88–90].

With \mathbf{n} and e_a^α defined, the integral form of the transport equation Eq. (10) can be evaluated using DIP over a phase space sub-domain $X_{\alpha\beta\gamma\delta} \times P_{ijk} = [t_\alpha, t_{\alpha+1}] \times [x_\beta, x_{\beta+1}] \times [y_\gamma, y_{\gamma+1}] \times [z_\delta, z_{\delta+1}] \times [p_i, p_{i+1}] \times [u_j, u_{j+1}] \times [\phi_k, \phi_{k+1}]$ to give the rather long expressions Eqs. (C2) to (C11) and (C13), found in Appendix C, whereby terms on the left hand side of Eq. (10) are converted into fluxes

at the boundaries of the sub-domain (see Fig. 7) and the right hand side has been converted into a series of collision arrays. These equations form a numerical evolution scheme for all particle distribution functions, including external forces and collisions between particles. Such a scheme is conservative in terms of the total number of particles in the system (in the absence of emissive processes which are free to add or subtract particles from the system), as fluxes are always balanced between sub-domains, i.e. any particles leaving one sub-domain of phase space enter another.

As an example of how these fluxes are generated, consider the the specific case of Schwarzschild geometry with coordinates $x^\alpha = \{t, r, \theta, \psi\}$ (see Appendix B). In this geometry $\mathbf{n} = -\sqrt{1 - \frac{r_s}{r}}\mathbf{dt}$, where r_s is the Schwarzschild radius, and the coordinate transformation Eq. (44) may be given by

$$e_a^\alpha = \begin{pmatrix} \frac{1}{\sqrt{1 - \frac{r_s}{r}}} & 0 & 0 & 0 \\ 0 & \sqrt{1 - \frac{r_s}{r}} & 0 & 0 \\ 0 & 0 & \frac{1}{r} & 0 \\ 0 & 0 & 0 & \frac{1}{r \sin \theta} \end{pmatrix}, \quad (45)$$

assuming the orthonormal basis vectors \mathbf{X} , \mathbf{Y} , and \mathbf{Z} are aligned to the global coordinate directions e_r , e_θ , and e_ϕ .

Using these definitions for the Eulerian observer \mathbf{n} and coordinate transformations e_a^α , the fluxes through phase space sub-domain boundaries and the spacetime volume element (Eqs. (C2) to (C11) and (C13)) can be evaluated analytically. For example, the flux elements $\mathcal{B}_{\alpha\beta\gamma\delta ijk}^+$ (Eq. (C4)) through boundaries of $r = \text{constant}$ are given by:

$$\mathcal{B}_{\alpha\beta\gamma\delta ijk}^+ = -\frac{1}{2} (t_{\alpha+1} - t_\alpha) \left(r_\beta^{3/2} \sqrt{r_\beta - r_s} \right) (\cos \theta_{\gamma+1} - \cos \theta_\gamma) (\psi_{\delta+1} - \psi_\delta) \left(\sqrt{m^2 + p_{i+1}^2} - \sqrt{m^2 + p_i^2} \right) \\ \times \left(u_{j+1} \sqrt{1 - u_{j+1}^2} - 2 \arccot \left(\frac{u_{j+1} - 1}{\sqrt{1 - u_{j+1}^2}} \right) - u_j \sqrt{1 - u_j^2} + 2 \arccot \left(\frac{u_j - 1}{\sqrt{1 - u_j^2}} \right) \right) (\sin \phi_{k+1} - \sin \phi_k). \quad (46)$$

Eq. (46) is not a particularly elegant expression but importantly it, and all other flux expressions, are independent of the distribution function and any state variables of the system. Therefore all terms relating to transport, fluxes and collisions, are pre-computable as fixed arrays.

V. CONCLUSION

This is the first paper in a series describing a novel mesoscopic framework for the general transport of particle distributions, with the aim of application to astrophysical systems.

In this paper, the transport of the particle distribution

through phase space has been described in a general manner. Continuous forces and discrete particle interactions have been included (Sections II and III).

This general description is independent of the underlying spacetime and agnostic to the types of particle interactions involved.

A novel approach of phase space discretisation of the particle distribution function, *Distribution-In-Plateaux* (Section IV), has been described that allows for the numerical evaluation of this transport in a conservative form.

Numerical implementation and microscopic testing of this approach is detailed in Paper II, with macroscopic tests to appear in Paper III.

It is planned to apply the DIPLODOCUS framework to AGN jet modelling in the future. In particular, the added dimensionality allowed by the relaxations of various assumptions on the particle distributions and jet geometries will be exploited. This will allow their effects on emission spectra to be examined and may provide insight into the jet content and particle acceleration mechanisms.

ACKNOWLEDGMENTS

C. N. Everett acknowledges an Science and Technologies Facilities Council (STFC) studentship

ST/X508664/1. G. Cotter acknowledges support from STFC grants ST/V006355/1, ST/V001477/1 and ST/S002952/1 and from Exeter College, Oxford. The authors would also like to thank James Matthews, Marc Klinger-Plaisier, Sera Markoff (and their research group), Pedro Ferreira, and Dion Everett for their helpful insights during various phases of this work.

DATA AVAILABILITY

No data were created or analysed in this article.

[1] C. M. Urry and P. Padovani, Unified Schemes for Radio-Loud Active Galactic Nuclei, *PASP* **107**, 803 (1995).

[2] P. Padovani, D. M. Alexander, R. J. Assef, B. D. Marco, P. Giommi, R. C. Hickox, G. T. Richards, V. Smolcic, E. Hatziminaoglou, V. Mainieri, and M. Salvato, Active Galactic Nuclei: what's in a name?, *Astron Astrophys Rev* **25**, 10.1007/s00159-017-0102-9 (2017).

[3] R. Blandford, D. Meier, and A. Readhead, Relativistic Jets from Active Galactic Nuclei, *Annual Review of Astronomy and Astrophysics* **57**, 467 (2019).

[4] J. C. McKinney and C. F. Gammie, A Measurement of the Electromagnetic Luminosity of a Kerr Black Hole, *ApJ* **611**, 977 (2004).

[5] J. C. McKinney, General relativistic magnetohydrodynamic simulations of the jet formation and large-scale propagation from black hole accretion systems, *Monthly Notices of the Royal Astronomical Society* **368**, 1561 (2006).

[6] K. Chatterjee, M. Liska, A. Tchekhovskoy, and S. B. Markoff, Accelerating AGN jets to parsec scales using general relativistic MHD simulations, *Monthly Notices of the Royal Astronomical Society* **490**, 2200 (2019).

[7] H. W. Whitehead and J. H. Matthews, Studying the link between radio galaxies and AGN fuelling with relativistic hydrodynamic simulations of flickering jets, *Mon Not R Astron Soc* **523**, 2478 (2023).

[8] B. Cerutti, G. R. Werner, D. A. Uzdensky, and M. C. Begelman, Simulations of Particle Acceleration beyond the Classical Synchrotron Burnoff Limit in Magnetic Reconnection: An Explanation of the Crab Flares, *The Astrophysical Journal* **770**, 147 (2013).

[9] L. Sironi, U. Keshet, and M. Lemoine, Relativistic Shocks: Particle Acceleration and Magnetization, *Space Sci Rev* **191**, 519 (2015).

[10] J. Mehlhaff, G. Werner, B. Cerutti, D. Uzdensky, and M. Begelman, Kinetic simulations and gamma-ray signatures of Klein-Nishina relativistic magnetic reconnection, *Monthly Notices of the Royal Astronomical Society* **527**, 11587 (2024).

[11] L. Comisso, G. R. Farrar, and M. S. Muzio, Ultra-High-Energy Cosmic Rays Accelerated by Magnetically Dominated Turbulence, *ApJL* **977**, L18 (2024).

[12] R. W. Lindquist, Relativistic transport theory, *Annals of Physics* **37**, 487 (1966).

[13] G. M. Webb, Relativistic Transport Theory for Cosmic Rays, *The Astrophysical Journal* **296**, 319 (1985).

[14] G. M. Webb, The diffusion approximation and transport theory for cosmic rays in relativistic flows, *The Astrophysical Journal* **340**, 1112 (1989).

[15] G. R. Blumenthal and R. J. Gould, Bremsstrahlung, Synchrotron Radiation, and Compton Scattering of High-Energy Electrons Traversing Dilute Gases, *Rev. Mod. Phys.* **42**, 237 (1970).

[16] T. A. Weaver, Reaction rates in a relativistic plasma, *Phys. Rev. A* **13**, 1563 (1976).

[17] F. A. Aharonian and A. M. Atoyan, Compton Scattering of Relativistic Electrons in Compact X-Ray Sources, *Astrophysics and Space Science* **79**, 321 (1981).

[18] R. Svensson, The pair annihilation process in relativistic plasmas, *The Astrophysical Journal* **258**, 321 (1982).

[19] M. Baring, Reaction rates and spectra in relativistic plasmas, *Monthly Notices of the Royal Astronomical Society* **228**, 681 (1987).

[20] C. D. Dermer, The production spectrum of a relativistic Maxwell-Boltzmann gas, *The Astrophysical Journal* **280**, 328 (1984).

[21] W. Brinkmann, Compton scattering from isotropic electrons, *Journal of Quantitative Spectroscopy and Radiative Transfer* **31**, 417 (1984).

[22] C. D. Dermer, Binary collision rates of relativistic thermal plasmas. I Theoretical framework, *The Astrophysical Journal* **295**, 28 (1985).

[23] C. D. Dermer, Binary Collision Rates of Relativistic Thermal Plasmas. II. Spectra, *The Astrophysical Journal* **307**, 47 (1986).

[24] P. S. Coppi and R. D. Blandford, Reaction rates and energy distributions for elementary processes in relativistic pair plasmas, *Monthly Notices of the Royal Astronomical Society* **245**, 453 (1990).

[25] A. Sarkar, J. Chluba, and E. Lee, Dissecting the Compton scattering kernel I: Isotropic media, *Monthly Notices of the Royal Astronomical Society* **490**, 3705 (2019).

[26] S. Stepney and P. W. Guilbert, Numerical fits to important rates in high temperature astrophysical plasmas, *Monthly Notices of the Royal Astronomical Society* **204**, 1269 (1983).

[27] I. V. Moskalenko and A. W. Strong, Anisotropic Inverse Compton Scattering in the Galaxy, *ApJ* **528**, 357 (2000).

[28] S. R. Kelner, E. Lefa, F. M. Rieger, and F. A. Aharonian, THE BEAMING PATTERN OF EXTERNAL COMPTON EMISSION FROM RELATIVISTIC OUTFLOWS: THE CASE OF ANISOTROPIC DISTRIBUTION OF

ELECTRONS, *ApJ* **785**, 141 (2014).

[29] A. C. M. Lai and K. C. Y. Ng, Anisotropic Photon and Electron Scattering without Ultrarelativistic Approximation, *Phys. Rev. D* **107**, 063026 (2023).

[30] C. N. Everett and G. Cotter, Computational forms for binary particle interactions at different levels of anisotropy, *RAS Techniques and Instruments* **3**, 548 (2024).

[31] A. Mastichiadis and J. G. Kirk, Self-consistent particle acceleration in active galactic nuclei., *Astronomy and Astrophysics* **295**, 613 (1995).

[32] A. Mastichiadis, R. J. Protheroe, and J. G. Kirk, Spectral and temporal signatures of ultrarelativistic protons in compact sources. I. Effects of Bethe-Heitler pair production, *Astronomy and Astrophysics* **433**, 765 (2005).

[33] S. Dimitrakoudis, A. Mastichiadis, R. J. Protheroe, and A. Reimer, The time-dependent one-zone hadronic model. First principles, *Astronomy and Astrophysics* **546**, A120 (2012).

[34] M. Böttcher, A. Reimer, K. Sweeney, and A. Prakash, Leptonic and Hadronic Modeling of Fermi-detected Blazars, *The Astrophysical Journal* **768**, 54 (2013).

[35] M. Petropoulou, D. Giannios, and S. Dimitrakoudis, Implications of a PeV neutrino spectral cut-off in gamma-ray burst models, *Monthly Notices of the Royal Astronomical Society* **445**, 570 (2014).

[36] M. Cerruti, A. Zech, C. Boisson, and S. Inoue, A hadronic origin for ultra-high-frequency-peaked BL Lac objects, *Monthly Notices of the Royal Astronomical Society* **448**, 910 (2015).

[37] S. Gao, M. Pohl, and W. Winter, On the Direct Correlation between Gamma-Rays and PeV Neutrinos from Blazars, *The Astrophysical Journal* **843**, 109 (2017).

[38] W. J. Potter, Modelling blazar flaring using a time-dependent fluid jet emission model – an explanation for orphan flares and radio lags, *Monthly Notices of the Royal Astronomical Society* **473**, 4107 (2018).

[39] B. Jiménez Fernández and H. van Eerten, Katu: a fast open-source full lepto-hadronic kinetic code suitable for Bayesian inference modelling of blazars (2021).

[40] M. Cerruti, M. Kreter, M. Petropoulou, A. Rudolph, F. Oikonomou, M. Böttcher, S. Dimitrakoudis, A. Dmytriiev, S. Gao, A. Mastichiadis, S. Inoue, K. Murase, A. Reimer, J. Robinson, X. Rodrigues, W. Winter, A. Zech, and N. Źywucka, *The Blazar Hadronic Code Comparison Project* (2021).

[41] S. Gasparyan, D. Bégué, and N. Sahakyan, Time-dependent lepto-hadronic modelling of the emission from blazar jets with SOPRANO: the case of TXS 0506 + 056, 3HSP J095507.9 + 355101, and 3C 279, *Monthly Notices of the Royal Astronomical Society* **509**, 2102 (2022).

[42] M. Zacharias, A. Reimer, C. Boisson, and A. Zech, ExHaLe-jet: an extended hadro-leptonic jet model for blazars – I. Code description and initial results, *Monthly Notices of the Royal Astronomical Society* **512**, 3948 (2022).

[43] J. Hahn, C. Romoli, and M. Breuhaus, GAMERA: Source modeling in gamma astronomy, *Astrophysics Source Code Library* , ascl:2203.007 (2022).

[44] M. Klinger, A. Rudolph, X. Rodrigues, C. Yuan, G. Fichet de Clairfontaine, A. Fedynitch, W. Winter, M. Pohl, and S. Gao, *AM³: An Open-Source Tool for Time-Dependent Lepto-Hadronic Modeling of Astrophysical Sources* (2023).

[45] S. I. Stathopoulos, M. Petropoulou, G. Vasilopoulos, and A. Mastichiadis, LeHaMoC: A versatile time-dependent lepto-hadronic modeling code for high-energy astrophysical sources, *A&A* **683**, A225 (2024).

[46] T. C. Weekes, *Very High Energy Gamma-Ray Astronomy*, Series in Astronomy and Astrophysics (Institute of Physics Pub., 2003).

[47] M. R. Hoerbe, P. J. Morris, G. Cotter, and J. B. Tjus, On the relative importance of hadronic emission processes along the jet axis of Active Galactic Nuclei, *Monthly Notices of the Royal Astronomical Society* **496**, 2885 (2020), 2006.05140.

[48] D. Kantzas, S. Markoff, M. Lucchini, C. Ceccobello, and K. Chatterjee, Exploring the role of composition and mass loading on the properties of hadronic jets, *Monthly Notices of the Royal Astronomical Society* **520**, 6017 (2023).

[49] S. Markoff, H. Falcke, and R. Fender, A jet model for the broadband spectrum of XTE J1118+480 - Synchrotron emission from radio to X-rays in the Low/Hard spectral state, *A&A* **372**, L25 (2001).

[50] A. P. Marscher, Turbulent, Extreme Multi-zone Model for Simulating Flux and Polarization Variability in Blazars, *The Astrophysical Journal* **780**, 87 (2014).

[51] W. J. Potter and G. Cotter, New constraints on the structure and dynamics of black hole jets, *Monthly Notices of the Royal Astronomical Society* **453**, 4070 (2015).

[52] D. Kantzas, S. Markoff, T. Beuchert, M. Lucchini, A. Chhotray, C. Ceccobello, A. J. Tetarenko, J. C. A. Miller-Jones, M. Bremer, J. A. Garcia, V. Grinberg, P. Uttley, and J. Wilms, A new lepto-hadronic model applied to the first simultaneous multiwavelength data set for Cygnus X-1, *Monthly Notices of the Royal Astronomical Society* **500**, 2112 (2021).

[53] M. Klinger, C. Yuan, A. M. Taylor, and W. Winter, *Lepto-Hadronic Scenarios for TeV Extensions of Gamma-Ray Burst Afterglow Spectra* (2024).

[54] A. G. Aksenov, M. Milgrom, and V. V. Usov, Structure of Pair Winds from Compact Objects with Application to Emission from Hot Bare Strange Stars, *ApJ* **609**, 363 (2004).

[55] A. G. Aksenov, R. Ruffini, and G. V. Vereshchagin, Thermalization of Nonequilibrium Electron-Positron-Photon Plasmas, *Phys. Rev. Lett.* **99**, 125003 (2007).

[56] A. G. Aksenov, R. Ruffini, and G. V. Vereshchagin, Pair plasma relaxation time scales, *Phys. Rev. E* **81**, 046401 (2010).

[57] M. R. Krumholz, R. M. Crocker, and M. L. Sampson, Cosmic ray interstellar propagation tool using Itô Calculus: software for simultaneous calculation of cosmic ray transport and observational signatures, *Monthly Notices of the Royal Astronomical Society* **517**, 1355 (2022).

[58] M. R. Krumholz, R. M. Crocker, A. Bahramian, and P. Bordas, Teraelectronvolt gamma-ray emission near globular cluster Terzan 5 as a probe of cosmic ray transport, *Nature Astronomy* **10**.1038/s41550-024-02337-1 (2024).

[59] C. N. Everett, M. Klinger-Plaisier, and G. Cotter, Diplodocus II: Implementation of transport equations and test cases relevant to micro-scale physics of jetted astrophysical sources (in prep.).

[60] C. N. Everett and G. Cotter, Diplodocus III: Test cases relevant to macro-scale physics of jetted astrophysical sources (in prep.).

[61] L. Boltzmann, Weitere Studien über das Wärmegleichgewicht unter Gas molekülen., *Sitzungsberichte der Kaiserlichen Akademie der Wissenschaften* **66**, 275 (1872).

[62] Ehlers, J, *General relativity and cosmology*, Its Proceedings, course 47 (Academic Press, New York, 1971).

[63] S. R. Groot, W. A. Leeuwen, and C. G. Weert, *Relativistic Kinetic Theory: Principles and Applications* (North-Holland Pub. Co., 1980).

[64] R. Hakim, Remarks on Relativistic Statistical Mechanics. I, *Journal of Mathematical Physics* **8**, 1315 (1967).

[65] R. Hakim, Remarks on Relativistic Statistical Mechanics. II. Hierarchies for the Reduced Densities, *Journal of Mathematical Physics* **8**, 1379 (1967).

[66] W. Steeb, Generalized liouville equation, entropy, and dynamic systems containing limit cycles, *Physica A: Statistical Mechanics and its Applications* **95**, 181 (1979).

[67] W. Steeb, A comment on the generalized Liouville equation, *Found Phys* **10**, 485 (1980).

[68] G. F. R. Ellis, D. R. Matravers, and R. Treciokas, Anisotropic solutions of the Einstein-Boltzmann equations: I. General formalism, *Annals of Physics* **150**, 455 (1983).

[69] G. F. R. Ellis, R. Treciokas, and D. R. Matravers, Anisotropic solutions of the Einstein-Boltzmann equations. II. Some exact properties of the equations, *Annals of Physics* **150**, 487 (1983).

[70] R. Blandford and D. Eichler, Particle acceleration at astrophysical shocks: A theory of cosmic ray origin, *Physics Reports* **154**, 1 (1987).

[71] C. Cercignani, *The relativistic Boltzmann equation: theory and applications*, Progress in mathematical physics, Vol. 22 (Birkhäuser, Basel, 2002).

[72] C. Y. Cardall and A. Mezzacappa, Conservative formulations of general relativistic kinetic theory, *Phys. Rev. D* **68**, 023006 (2003).

[73] E. M. Lifshits, *Physical kinetics*, Course of theoretical physics ; v. 10 (Elsevier, 2008).

[74] M. Shibata, H. Nagakura, Y. Sekiguchi, and S. Yamada, Conservative form of Boltzmann's equation in general relativity, *Phys. Rev. D* **89**, 084073 (2014).

[75] E. Cartan, *Leçons sur les invariants intégraux* (Hermann, 1922).

[76] F. Hélein, Answer to "Is "Cartan's magic formula" due to Élie or Henri?" (2023).

[77] T. De Donder, Sur les invariants intégraux relatifs et leurs applications à la physique mathématique, *Bulletin de la Classe des sciences. Académie royale de Belgique* , 50 (1911).

[78] S. M. Stigler, Stigler's Law of Eponymy, *Transactions of the New York Academy of Sciences* **39**, 147 (1980).

[79] J. Liouville, Note sur la Théorie de la Variation des constantes arbitraires., *Journal de Mathématiques Pures et Appliquées* , 342 (1838).

[80] M. Abraham, *Theorie der elektrizität. Zweiter Band: Elektromagnetische Theorie der Strahlung* (B.G. Teubner, Leipzig, 1905).

[81] H. A. Lorentz, *La théorie électromagnétique de Maxwell et son application aux corps mouvants par H.A. Lorentz* (E.J. Brill, Netherlands, 1892).

[82] P. A. M. Dirac, Classical theory of radiating electrons, *Proceedings of the Royal Society of London. Series A. Mathematical and Physical Sciences* **167**, 148 (1938).

[83] S. E. Gralla, A. I. Harte, and R. M. Wald, Rigorous derivation of electromagnetic self-force, *Phys. Rev. D* **80**, 024031 (2009).

[84] E. Poisson, A. Pound, and I. Vega, The Motion of Point Particles in Curved Spacetime, *Living Rev. Relativ.* **14**, 7 (2011).

[85] V. B. Berestetskii, E. M. Lifshits, and L. P. Pitaevskii, *Quantum Electrodynamics*, 2nd ed. (Butterworth-Heinemann, 1982).

[86] B. Cockburn and C.-W. Shu, Runge–Kutta Discontinuous Galerkin Methods for Convection-Dominated Problems, *Journal of Scientific Computing* **16**, 173 (2001).

[87] I. M. Gamba and S. Rjasanow, Galerkin–Petrov approach for the Boltzmann equation, *Journal of Computational Physics* **366**, 341 (2018).

[88] A. Chael, A. Lupsasca, G. N. Wong, and E. Quataert, Black Hole Polarimetry I: A Signature of Electromagnetic Energy Extraction, *ApJ* **958**, 65 (2023).

[89] Z. Gelles, A. Chael, and E. Quataert, Signatures of Black Hole Spin and Plasma Acceleration in Jet Polarimetry, *ApJ* **981**, 204 (2025).

[90] Y. Tsunetoe, D. W. Pesce, R. Narayan, A. Chael, Z. Gelles, C. F. Gammie, E. Quataert, and D. C. M. Palumbo, Limb-Brightened Jet in M87 from Anisotropic Nonthermal Electrons (2025).

Appendix A: Collision Integral for Binary and Emissive interactions

1. Binary Interactions

Consider the reversible binary (scattering) interaction $\mathbf{ab} \rightleftharpoons \mathbf{cd}$. The collision integral for a particle of type-c in this interaction is given by Eq. (36):

$$C(\mathbf{x}, \mathbf{p}_c) = N_{\mathbf{ab} \rightarrow \mathbf{cd}} - N_{\mathbf{ab} \leftarrow \mathbf{cd}} \quad (\text{A1})$$

$N_{\mathbf{ab} \rightarrow \mathbf{cd}}$ is the number of worldlines created by the forward interaction $\mathbf{ab} \rightarrow \mathbf{cd}$ in this reversible process, hence giving the number of particle type-c (and type-d) worldlines started by that interaction within a volume of phase space. Using Eq. (35) this may be written

$$N_{\mathbf{ab} \rightarrow \mathbf{cd}} = \delta^{(4)}(\mathbf{p}_a + \mathbf{p}_b - \mathbf{p}_c - \mathbf{p}_d) |M_{\mathbf{ab} \rightarrow \mathbf{cd}}|^2 f_a(\mathbf{x}, \mathbf{p}_a) f_b(\mathbf{x}, \mathbf{p}_b) \frac{\pi_a \pi_b}{(1 + \delta_{ab})} \frac{\pi_c \pi_d}{(1 + \delta_{cd})} \chi. \quad (\text{A2})$$

Three of the Dirac delta functions in above equation can be removed by integrating over the momentum states of the other output particle in the interaction, i.e. states of type- \mathfrak{d} particles

$$N_{\mathfrak{a}\mathfrak{b} \rightarrow \mathfrak{c}\mathfrak{d}} = \delta(p_{\mathfrak{a}}^0 + p_{\mathfrak{b}}^0 - p_{\mathfrak{c}}^0 - p_{\mathfrak{d}}^0) |M_{\mathfrak{a}\mathfrak{b} \rightarrow \mathfrak{c}\mathfrak{d}}|^2 f_{\mathfrak{a}}(\mathbf{x}, \mathbf{p}_{\mathfrak{a}}) f_{\mathfrak{b}}(\mathbf{x}, \mathbf{p}_{\mathfrak{b}}) \frac{d^3 p_{\mathfrak{a}} d^3 p_{\mathfrak{b}}}{p_{\mathfrak{a}}^0 p_{\mathfrak{b}}^0 (1 + \delta_{\mathfrak{a}\mathfrak{b}})} \frac{d^3 p_{\mathfrak{c}}}{p_{\mathfrak{c}}^0 p_{\mathfrak{d}}^0 (1 + \delta_{\mathfrak{c}\mathfrak{d}})} \chi, \quad (\text{A3})$$

where $p_{\mathfrak{d}}^0$ is now a function of the other particle momenta given by energy conservation $p_{\mathfrak{d}}^0 = p_{\mathfrak{a}}^0 + p_{\mathfrak{b}}^0 - p_{\mathfrak{c}}^0$ and note the shorthand for the momentum space volume element $\frac{d^3 p}{p^0} = \frac{(p)^2 dp dud\phi}{p^0} = \frac{dp^1 \wedge dp^2 \wedge dp^3}{p^0}$.

For binary collisions, the rate is typically measured using a differential cross section. For generality of reference frame, it is best to use the Lorentz invariant differential cross section $\frac{d\sigma_{\mathfrak{a}\mathfrak{b} \rightarrow \mathfrak{c}\mathfrak{d}}}{dT}$, which is a function of the the standard Mandelstam variables S, T and U . This differential cross section can be related to the scattering matrix (Eq. (33)) by

$$|M_{\mathfrak{a}\mathfrak{b} \rightarrow \mathfrak{c}\mathfrak{d}}|^2 = \frac{\mathcal{F}_{\mathfrak{a}\mathfrak{b}}^2}{\pi} \frac{d\sigma_{\mathfrak{a}\mathfrak{b} \rightarrow \mathfrak{c}\mathfrak{d}}}{dT}, \quad (\text{A4})$$

where $\mathcal{F}_{\mathfrak{a}\mathfrak{b}} = \frac{1}{2} \sqrt{(S - (m_{\mathfrak{a}} + m_{\mathfrak{b}})^2)(S - (m_{\mathfrak{a}} - m_{\mathfrak{b}})^2)}$ is a Lorentz scalar related to the incident flux of particles of type- \mathfrak{a} and type- \mathfrak{b} .

The internal terms of Eq. (A3) may then be collected into the expression

$$N_{\mathfrak{a}\mathfrak{b} \rightarrow \mathfrak{c}\mathfrak{d}} = f_{\mathfrak{a}}(\mathbf{x}, \mathbf{p}_{\mathfrak{a}}) f_{\mathfrak{b}}(\mathbf{x}, \mathbf{p}_{\mathfrak{b}}) G_{\mathfrak{a}\mathfrak{b} \rightarrow \mathfrak{c}\mathfrak{d}} d^3 p_{\mathfrak{a}} d^3 p_{\mathfrak{b}} d^3 p_{\mathfrak{c}} \chi, \quad G_{\mathfrak{a}\mathfrak{b} \rightarrow \mathfrak{c}\mathfrak{d}} = \frac{\delta(p_{\mathfrak{a}}^0 + p_{\mathfrak{b}}^0 - p_{\mathfrak{c}}^0 - p_{\mathfrak{d}}^0)}{(1 + \delta_{\mathfrak{a}\mathfrak{b}})(1 + \delta_{\mathfrak{c}\mathfrak{d}})} \frac{\mathcal{F}_{\mathfrak{a}\mathfrak{b}}^2}{\pi p_{\mathfrak{a}}^0 p_{\mathfrak{b}}^0 p_{\mathfrak{c}}^0 p_{\mathfrak{d}}^0} \frac{d\sigma_{\mathfrak{a}\mathfrak{b} \rightarrow \mathfrak{c}\mathfrak{d}}}{dT}, \quad (\text{A5})$$

with $G_{\mathfrak{a}\mathfrak{b} \rightarrow \mathfrak{c}\mathfrak{d}}$ being denoted the “gain term” of particles of type- \mathfrak{c} (and type- \mathfrak{d}) for the forward reaction.

For the reverse process $N_{\mathfrak{a}\mathfrak{b} \leftarrow \mathfrak{c}\mathfrak{d}}$, Eq. (A5) can be altered and simplified by acknowledging that now both output states (now particles of type- \mathfrak{a} and type- \mathfrak{b}) can be integrated over, leading to

$$N_{\mathfrak{a}\mathfrak{b} \leftarrow \mathfrak{c}\mathfrak{d}} = f_{\mathfrak{c}}(\mathbf{x}, \mathbf{p}_{\mathfrak{c}}) f_{\mathfrak{d}}(\mathbf{x}, \mathbf{p}_{\mathfrak{d}}) L_{\mathfrak{a}\mathfrak{b} \leftarrow \mathfrak{c}\mathfrak{d}} d^3 p_{\mathfrak{c}} d^3 p_{\mathfrak{d}} \chi, \quad L_{\mathfrak{a}\mathfrak{b} \leftarrow \mathfrak{c}\mathfrak{d}} = \frac{1}{(1 + \delta_{\mathfrak{c}\mathfrak{d}})} \frac{\mathcal{F}_{\mathfrak{c}\mathfrak{d}} \sigma_{\mathfrak{a}\mathfrak{b} \leftarrow \mathfrak{c}\mathfrak{d}}}{p_{\mathfrak{c}}^0 p_{\mathfrak{d}}^0}, \quad (\text{A6})$$

where $\sigma_{\mathfrak{a}\mathfrak{b} \leftarrow \mathfrak{c}\mathfrak{d}}$ is the Lorentz invariant total cross section for the reverse process $\mathfrak{a}\mathfrak{b} \leftarrow \mathfrak{c}\mathfrak{d}$, which typically involves the factor of $1/(1 + \delta_{\mathfrak{a}\mathfrak{b}})$ in its evaluation, and $L_{\mathfrak{a}\mathfrak{b} \leftarrow \mathfrak{c}\mathfrak{d}}$ is the “loss term” for particles of type- \mathfrak{c} (and type- \mathfrak{d}) for the reverse reaction.

2. Binary Interactions in DIP Form

Under the assumption that the distribution function take the form granted by DIP, Eq. (37), the gain and loss terms Eqs. (A5) and (A6) may be integrated over sub-domains of the momentum space of the particles involved to give the “gain array” components:

$$G_{\mathfrak{a}\mathfrak{b} \rightarrow \mathfrak{c}\mathfrak{d},ijklmnopq} = \int_{P_{ijk}} \int_{P_{lmn}} \int_{P_{opq}} G_{\mathfrak{a}\mathfrak{b} \rightarrow \mathfrak{c}\mathfrak{d}} \frac{d^3 p_{\mathfrak{b}}}{(p_{\mathfrak{b}})^2 \Delta p_{\mathfrak{b},o} \Delta u_{\mathfrak{b},p} \Delta \phi_{\mathfrak{b},q}} \frac{d^3 p_{\mathfrak{a}}}{(p_{\mathfrak{a}})^2 \Delta p_{\mathfrak{a},l} \Delta u_{\mathfrak{a},m} \Delta \phi_{\mathfrak{a},n}} d^3 p_{\mathfrak{c}} \quad (\text{A7})$$

and “loss array” components

$$L_{\mathfrak{a}\mathfrak{b} \leftarrow \mathfrak{c}\mathfrak{d},ijklmn} = \int_{P_{ijk}} \int_{P_{lmn}} L_{\mathfrak{a}\mathfrak{b} \leftarrow \mathfrak{c}\mathfrak{d}} \frac{d^3 p_{\mathfrak{d}}}{(p_{\mathfrak{d}})^2 \Delta p_{\mathfrak{d},l} \Delta u_{\mathfrak{d},m} \Delta \phi_{\mathfrak{d},n}} \frac{d^3 p_{\mathfrak{c}}}{(p_{\mathfrak{c}})^2 \Delta p_{\mathfrak{c},i} \Delta u_{\mathfrak{c},j} \Delta \phi_{\mathfrak{c},k}} \quad (\text{A8})$$

which are pre-computable by numerical methods (see [Paper II](#)) and independent of spatial coordinates, as such are valid at any point in space.

3. Emissive Interactions

Consider an emissive interaction where one particle “decays” into two $\mathfrak{a} \rightarrow \mathfrak{b}\mathfrak{c}$. The collision integral for a particle of type- \mathfrak{c} in this interaction is given by Eq. (36):

$$C(\mathbf{x}, \mathbf{p}_{\mathfrak{c}}) = N_{\mathfrak{a} \rightarrow \mathfrak{b}\mathfrak{c}}, \quad (\text{A9})$$

$N_{a \rightarrow bc}$ is the number of worldline of particles of type- c created by the emissive interaction for $a \rightarrow bc$. Using Eq. (35) this may be written:

$$N_{a \rightarrow bc} = \delta^{(4)}(\mathbf{p}_a - \mathbf{p}_b - \mathbf{p}_c) |M_{a \rightarrow bc}|^2 f_a(\mathbf{x}, \mathbf{p}_a) \pi_a \frac{\pi_b \pi_c}{(1 + \delta_{bc})} \chi. \quad (\text{A10})$$

Three of the Dirac delta functions in the above equation can be removed by integrating over the momentum states of the outgoing particle of type- b :

$$N_{a \rightarrow bc} = \frac{\delta(p_a^0 - p_b^0 - p_c^0) |M_{a \rightarrow bc}|^2}{p_a^0 p_b^0 p_c^0 (1 + \delta_{bc})} f_a(\mathbf{x}, \mathbf{p}_a) d^3 p_a d^3 p_c \chi = \frac{dN_{a \rightarrow bc}}{dx^0 d^3 p_c} f_a(\mathbf{x}, \mathbf{p}_a) d^3 p_a d^3 p_c \chi, \quad (\text{A11})$$

where $\frac{dN_{a \rightarrow bc}}{dx^0 d^3 p_c}$ is the single particle emissivity of the interaction. This single particle emissivity is typically dependent on some external field such as the presence of a magnetic field in the case of synchrotron emissions.

4. Emissive Interactions in DIP Form

Under the assumptions that the distribution of the particles takes the form granted by DIP, Eq. (37), the gain array for an emissive interaction $a \rightarrow bc$ can be generated by integrating Eq. (A11) over discrete sub-domains of momentum space:

$$G_{a \rightarrow bc, i j k l m n} = \int_{P_{ijk}} \int_{P_{lmn}} G_{a \rightarrow bc} \frac{d^3 p_a}{(p_a)^2 \Delta p_{a,i} \Delta u_{a,m} \Delta \phi_{a,n}} \frac{d^3 p_c}{(p_c)^2}, \quad G_{a \rightarrow bc} = (p_c)^2 \frac{dN_{a \rightarrow bc}}{dx^0 d^3 p_c} \quad (\text{A12})$$

Appendix B: Metrics

A metric of the form Eq. (42), can express most standard astrophysically relevant metrics. A subset are presented below:

- Cartesian Minkowski:
 $x^\alpha = \{t, x, y, z\}, A^2 = 1, B^2 = 1, C^2 = 1, D^2 = 1, E = F = G = 0$
- Spherical Minkowski:
 $x^\alpha = \{t, r, \theta, \psi\}, A^2 = 1, B^2 = 1, C^2 = r^2, D^2 = r^2 \sin^2 \theta, E = F = G = 0$
- Cylindrical Minkowski:
 $x^\alpha = \{t, \rho, \vartheta, z\}, A^2 = 1, B^2 = 1, C^2 = \rho^2, D^2 = 1, E = F = G = 0$
- Schwarzschild:
 $x^\alpha = \{t, r, \theta, \psi\}, A^2 = (1 - \frac{r_s}{r}), B^2 = (1 - \frac{r_s}{r})^{-1}, C^2 = r^2, D^2 = r^2 \sin^2 \theta, E = F = G = 0$
- Kerr (Boyer-Lindquist Coordinates):
 $x^\alpha = \{t, r, \theta, \psi\}, A^2 = (1 - \frac{r_s}{r}), B^2 = \frac{\Sigma}{\Delta}, C^2 = \Sigma, D^2 = \left(r^2 + a^2 + \frac{r_s r a^2}{\Sigma} \sin^2 \theta\right) \sin^2 \theta, E = F = 0,$
 $G = \frac{-r_s r a \sin^2 \theta}{\Sigma}, \Sigma = r^2 + a^2 \cos^2 \theta, \Delta = r^2 - r r_s + a^2$

Appendix C: DIP Transport Equations

Under the assumption that the distribution function $f(\mathbf{x}, \mathbf{p})$ for all particles takes the DIP form, Eq. (37), the integral form of the transport equation Eq. (10), for a particle of type- c can be evaluated over a phase-space sub-domain $X_{\alpha\beta\gamma\delta} \times P_{ijk} = [t_\alpha, t_{\alpha+1}] \times [x_\beta, x_{\beta+1}] \times [y_\gamma, y_{\gamma+1}] \times [z_\delta, z_{\delta+1}] \times [p_i, p_{i+1}] \times [u_j, u_{j+1}] \times [\phi_k, \phi_{k+1}]$ to give the

discrete DIP transport equation:

$$\begin{aligned}
& (h_{\alpha+1}^- f_{\mathfrak{c},(\alpha+1)\beta\gamma\delta ijk} + h_\alpha^+ f_{\mathfrak{c},\alpha\beta\gamma\delta ijk}) \mathcal{A}_{\alpha\beta\gamma\delta ijk}^+ + (h_\alpha^- f_{\mathfrak{c},\alpha\beta\gamma\delta ijk} + h_{\alpha-1}^+ f_{\mathfrak{c},(\alpha-1)\beta\gamma\delta ijk}) \mathcal{A}_{\alpha\beta\gamma\delta ijk}^- \\
& + (h_{\beta+1}^- f_{\mathfrak{c},\alpha(\beta+1)\gamma\delta ijk} - h_\beta^+ f_{\mathfrak{c},\alpha\beta\gamma\delta ijk}) \mathcal{B}_{\alpha\beta\gamma\delta ijk}^+ + (h_\beta^- f_{\mathfrak{c},\alpha\beta\gamma\delta ijk} - h_{\beta-1}^+ f_{\mathfrak{c},\alpha(\beta-1)\gamma\delta ijk}) \mathcal{B}_{\alpha\beta\gamma\delta ijk}^- \\
& + (h_{\gamma+1}^- f_{\mathfrak{c},\alpha\beta(\gamma+1)\delta ijk} + h_\gamma^+ f_{\mathfrak{c},\alpha\beta\gamma\delta ijk}) \mathcal{C}_{\alpha\beta\gamma\delta ijk}^+ + (h_\gamma^- f_{\mathfrak{c},\alpha\beta\gamma\delta ijk} + h_{\gamma-1}^+ f_{\mathfrak{c},\alpha\beta(\gamma-1)\delta ijk}) \mathcal{C}_{\alpha\beta\gamma\delta ijk}^- \\
& + (h_{\delta+1}^- f_{\mathfrak{c},\alpha\beta\gamma(\delta+1)ijk} + h_\delta^+ f_{\mathfrak{c},\alpha\beta\gamma\delta ijk}) \mathcal{D}_{\alpha\beta\gamma\delta ijk}^+ + (h_\delta^- f_{\mathfrak{c},\alpha\beta\gamma\delta ijk} + h_{\delta-1}^+ f_{\mathfrak{c},\alpha\beta\gamma(\delta-1)ijk}) \mathcal{D}_{\alpha\beta\gamma\delta ijk}^- \\
& + \left(\frac{h_{i+1}^- f_{\mathfrak{c},\alpha\beta\gamma\delta(i+1)jk}}{\Delta p_{\mathfrak{c},i+1}} + \frac{h_i^+ f_{\mathfrak{c},\alpha\beta\gamma\delta ijk}}{\Delta p_{\mathfrak{c},i}} \right) \mathcal{I}_{\alpha\beta\gamma\delta ijk}^+ + \left(\frac{h_i^- f_{\mathfrak{c},\alpha\beta\gamma\delta ijk}}{\Delta p_{\mathfrak{c},i}} + \frac{h_{i-1}^+ f_{\mathfrak{c},\alpha\beta\gamma\delta(i-1)jk}}{\Delta p_{\mathfrak{c},i-1}} \right) \mathcal{I}_{\alpha\beta\gamma\delta ijk}^- \\
& + \left(\frac{h_{j+1}^- f_{\mathfrak{c},\alpha\beta\gamma\delta i(j+1)k}}{\Delta u_{\mathfrak{c},j+1}} + \frac{h_j^+ f_{\mathfrak{c},\alpha\beta\gamma\delta ijk}}{\Delta u_{\mathfrak{c},j}} \right) \mathcal{J}_{\alpha\beta\gamma\delta ijk}^+ + \left(\frac{h_j^- f_{\mathfrak{c},\alpha\beta\gamma\delta ijk}}{\Delta u_{\mathfrak{c},j}} + \frac{h_{j-1}^+ f_{\mathfrak{c},\alpha\beta\gamma\delta i(j-1)k}}{\Delta u_{\mathfrak{c},j-1}} \right) \mathcal{J}_{\alpha\beta\gamma\delta ijk}^- \\
& + \left(\frac{h_{k+1}^- f_{\mathfrak{c},\alpha\beta\gamma\delta i(j+1)k}}{\Delta \phi_{\mathfrak{c},k+1}} + \frac{h_k^+ f_{\mathfrak{c},\alpha\beta\gamma\delta ijk}}{\Delta \phi_{\mathfrak{c},k}} \right) \mathcal{K}_{\alpha\beta\gamma\delta ijk}^+ + \left(\frac{h_k^- f_{\mathfrak{c},\alpha\beta\gamma\delta ijk}}{\Delta \phi_{\mathfrak{c},k}} + \frac{h_{k-1}^+ f_{\mathfrak{c},\alpha\beta\gamma\delta i(j-1)k}}{\Delta \phi_{\mathfrak{c},k-1}} \right) \mathcal{K}_{\alpha\beta\gamma\delta ijk}^- \\
& = \sum_{\mathfrak{ab}\mathfrak{d} \in \text{particles}} \left(\sum_{lmnopq} G_{\mathfrak{ab} \rightarrow \mathfrak{cd}, i j k l m n o p q} f_{\mathfrak{a}, \alpha\beta\gamma\delta l m n} f_{\mathfrak{b}, \alpha\beta\gamma\delta o p q} - \sum_{lmn} L_{\mathfrak{ab} \leftarrow \mathfrak{cd}, i j k l m n} f_{\mathfrak{c}, \alpha\beta\gamma\delta i j k} f_{\mathfrak{d}, \alpha\beta\gamma\delta l m n} \right) \mathcal{V}_{\alpha\beta\gamma\delta} \\
& + \sum_{\mathfrak{ab} \in \text{particles}} \sum_{lmn} G_{\mathfrak{a} \rightarrow \mathfrak{b}\mathfrak{c}, i j k l m n} f_{\mathfrak{a}, \alpha\beta\gamma\delta l m n} \mathcal{V}_{\alpha\beta\gamma\delta}
\end{aligned} \tag{C1}$$

where the fluxes through hypersurfaces of constant time coordinate are:

$$\mathcal{A}_{\alpha\beta\gamma\delta ijk}^+ = \int_{\phi_k}^{\phi_{k+1}} \int_{u_j}^{u_{j+1}} \int_{p_i}^{p_{i+1}} \int_{z_\delta}^{z_{\delta+1}} \int_{y_\gamma}^{y_{\gamma+1}} \int_{x_\beta}^{x_{\beta+1}} \left[p^a e_a^0 \frac{\chi_{0123}}{p^0} \right]_{t_{\alpha+1}} \frac{dx dy dz dp du d\phi}{\Delta p_i \Delta u_j \Delta \phi_k}, \tag{C2}$$

$$\mathcal{A}_{\alpha\beta\gamma\delta ijk}^- = -\mathcal{A}_{(\alpha-1)\beta\gamma\delta ijk}^+, \tag{C3}$$

the fluxes through hypersurfaces of constant spatial coordinates are:

$$\mathcal{B}_{\alpha\beta\gamma\delta ijk}^+ = \int_{\phi_k}^{\phi_{k+1}} \int_{u_j}^{u_{j+1}} \int_{p_i}^{p_{i+1}} \int_{t_\alpha}^{t_{\alpha+1}} \int_{z_\delta}^{z_{\delta+1}} \int_{y_\gamma}^{y_{\gamma+1}} \left[p^a e_a^1 \frac{\chi_{1230}}{p^0} \right]_{x_{\beta+1}} \frac{dy dz dt dp du d\phi}{\Delta p_i \Delta u_j \Delta \phi_k}, \tag{C4}$$

$$\mathcal{C}_{\alpha\beta\gamma\delta ijk}^+ = \int_{\phi_k}^{\phi_{k+1}} \int_{u_j}^{u_{j+1}} \int_{p_i}^{p_{i+1}} \int_{x_\beta}^{x_{\beta+1}} \int_{t_\alpha}^{t_{\alpha+1}} \int_{z_\delta}^{z_{\delta+1}} \left[p^a e_a^2 \frac{\chi_{2301}}{p^0} \right]_{y_{\gamma+1}} \frac{dz dt dx dp du d\phi}{\Delta p_i \Delta u_j \Delta \phi_k}, \tag{C5}$$

$$\mathcal{D}_{\alpha\beta\gamma\delta ijk}^+ = \int_{\phi_k}^{\phi_{k+1}} \int_{u_j}^{u_{j+1}} \int_{p_i}^{p_{i+1}} \int_{y_\gamma}^{y_{\gamma+1}} \int_{x_\beta}^{x_{\beta+1}} \int_{t_\alpha}^{t_{\alpha+1}} \left[p^a e_a^3 \frac{\chi_{3012}}{p^0} \right]_{z_{\delta+1}} \frac{dt dx dy dp du d\phi}{\Delta p_i \Delta u_j \Delta \phi_k}, \tag{C6}$$

$$\mathcal{B}_{\alpha\beta\gamma\delta ijk}^- = -\mathcal{B}_{(\beta-1)\gamma\delta ijk}^+, \quad \mathcal{C}_{\alpha\beta\gamma\delta ijk}^- = -\mathcal{C}_{\alpha\beta(\gamma-1)\delta ijk}^+, \quad \mathcal{D}_{\alpha\beta\gamma\delta ijk}^- = -\mathcal{D}_{\alpha\beta\gamma(\delta-1)ijk}^+, \tag{C7}$$

the fluxes through constant momentum coordinates are:

$$\mathcal{I}_{\alpha\beta\gamma\delta ijk}^+ = \int_{\phi_k}^{\phi_{k+1}} \int_{u_j}^{u_{j+1}} \int_{z_\delta}^{z_{\delta+1}} \int_{y_\gamma}^{y_{\gamma+1}} \int_{x_\beta}^{x_{\beta+1}} \int_{t_\alpha}^{t_{\alpha+1}} \left[\frac{\chi_{0123}}{p^0} R_a^1 (-\Gamma_{bc}^a p^b p^c + m F^a) \right]_{p_{i+1}} \frac{dt dx dy dz du d\phi}{\Delta u_j \Delta \phi_k}, \tag{C8}$$

$$\mathcal{J}_{\alpha\beta\gamma\delta ijk}^+ = \int_{p_i}^{p_{i+1}} \int_{\phi_k}^{\phi_{k+1}} \int_{z_\delta}^{z_{\delta+1}} \int_{y_\gamma}^{y_{\gamma+1}} \int_{x_\beta}^{x_{\beta+1}} \int_{t_\alpha}^{t_{\alpha+1}} \left[\frac{\chi_{0123}}{p^0} R_a^2 (-\Gamma_{bc}^a p^b p^c + m F^a) \right]_{u_{j+1}} \frac{dt dx dy dz d\phi dp}{\Delta p_i \Delta \phi_k}, \tag{C9}$$

$$\mathcal{K}_{\alpha\beta\gamma\delta ijk}^+ = \int_{u_j}^{u_{j+1}} \int_{p_i}^{p_{i+1}} \int_{z_\delta}^{z_{\delta+1}} \int_{y_\gamma}^{y_{\gamma+1}} \int_{x_\beta}^{x_{\beta+1}} \int_{t_\alpha}^{t_{\alpha+1}} \left[\frac{\chi_{0123}}{p^0} R_a^3 (-\Gamma_{bc}^a p^b p^c + m F^a) \right]_{\phi_{k+1}} \frac{dt dx dy dz dp du}{\Delta p_i \Delta u_j}, \tag{C10}$$

$$\mathcal{I}_{\alpha\beta\gamma\delta ijk}^- = -\mathcal{I}_{\alpha\beta\gamma\delta(i-1)jk}^+, \quad \mathcal{J}_{\alpha\beta\gamma\delta ijk}^- = -\mathcal{J}_{\alpha\beta\gamma\delta i(j-1)k}^+, \quad \mathcal{K}_{\alpha\beta\gamma\delta ijk}^- = -\mathcal{K}_{\alpha\beta\gamma\delta i(j-1)k}^+, \tag{C11}$$

with $p^a = (p^0, p\sqrt{1-u^2} \cos \phi, p\sqrt{1-u^2} \sin \phi, pu)$ in modified spherical coordinates, with the associated transformation for vector components

$$R_a^b = \begin{pmatrix} 1 & 0 & 0 & 0 \\ 0 & \sqrt{1-u^2} \cos \phi & \sqrt{1-u^2} \sin \phi & u \\ 0 & -\frac{u\sqrt{1-u^2} \cos \phi}{p} & -\frac{u\sqrt{1-u^2} \sin \phi}{p} & \frac{1-u^2}{p} \\ 0 & -\frac{\sin \phi}{p\sqrt{1-u^2}} & \frac{\cos \phi}{p\sqrt{1-u^2}} & 0 \end{pmatrix}, \tag{C12}$$

and the spacetime volume element is

$$\mathcal{V}_{\alpha\beta\gamma\delta} = \int_{z_\delta}^{z_{\delta+1}} \int_{y_\gamma}^{y_{\gamma+1}} \int_{x_\beta}^{x_{\beta+1}} \int_{t_\alpha}^{t_{\alpha+1}} \chi_{0123} dt dx dy dz. \quad (\text{C13})$$

The fluxes and volume elements (Eqs. (C2) to (C11) and (C13)) are all integrals over phase-space sub-domains, which in most cases can be analytically integrated as the form of all the internal functions, connection coefficients, external forces etc. are known (see, for example, Eq. (46)).